

# Unraveling the predictive role of temperature in the gut microbiota of the sea urchin *Echinometra* sp. EZ across spatial and temporal gradients

Remi N. Ketchum<sup>1</sup>  | Edward G. Smith<sup>1,2</sup>  | Grace O. Vaughan<sup>2</sup> | Dain McParland<sup>2</sup> |  
Noura Al-Mansoori<sup>2</sup> | John A. Burt<sup>2</sup>  | Adam M. Reitzel<sup>1</sup> 

<sup>1</sup>Department of Biological Sciences,  
University of North Carolina at Charlotte,  
Charlotte, NC, USA

<sup>2</sup>Water Research Center & Center for  
Genomics and Systems Biology, New York  
University Abu Dhabi, Abu Dhabi, UAE

#### Correspondence

Remi N. Ketchum, Department of  
Biological Sciences, University of North  
Carolina at Charlotte, Charlotte, NC, USA.  
Email: rketchu1@uncc.edu

#### Funding information

ICRS Fellowship; NSF, Grant/Award  
Number: 1924498; NYUAD Water  
Research Center, Grant/Award Number:  
CG007; NSF GRF; Incentive Funds

## Abstract

Shifts in microbial communities represent a rapid response mechanism for host organisms to respond to changes in environmental conditions. Therefore, they are likely to be important in assisting the acclimatization of hosts to seasonal temperature changes as well as to variation in temperatures across a species' range. The Persian/Arabian Gulf is the world's warmest sea, with large seasonal fluctuations in temperature (20°C - 37°C) and is connected to the Gulf of Oman which experiences more typical oceanic conditions (<32°C in the summer). This system is an informative model for understanding how symbiotic microbial assemblages respond to thermal variation across temporal and spatial scales. Here, we elucidate the role of temperature on the microbial gut community of the sea urchin *Echinometra* sp. EZ and identify microbial taxa that are tightly correlated with the thermal environment. We generated two independent datasets with a high degree of geographic and temporal resolution. The results show that microbial communities vary across thermally variable habitats, display temporal shifts that correlate with temperature, and can become more disperse as temperatures rise. The relative abundances of several ASVs significantly correlate with temperature in both independent datasets despite the >300 km distance between the furthest sites and the extreme seasonal variations. Notably, over 50% of the temperature predictive ASVs identified from the two datasets belonged to the family Vibrionaceae. Together, our results identify temperature as a robust predictor of community-level variation and highlight specific microbial taxa putatively involved in the response to thermal environment.

#### KEY WORDS

*Echinometra*, gut microbiota, microbial ecology, Persian/Arabian Gulf, sea urchin, thermal gradient

## 1 | INTRODUCTION

The microbiome is important in shaping organismal biology in a wide range of eukaryotic species and has been shown to play critical roles

in host physiological functions and susceptibility to disease (Bayer et al., 2008; Gatesoupe, 1999; Hentschel et al., 2012). Research describing the distribution, structure, and function of the microbiome has flourished in the last decade, and in marine habitats these studies

have generally focused on species important for ecosystem function, including corals (Hadadi et al., 2017; Ziegler et al., 2019), sponges (Reveillaud et al., 2014), macroalgae (Thurber et al., 2012), seagrasses (Hurtado-McCormick et al., 2019), sea urchins (Carrier et al., 2020), and mangroves (Lin et al., 2019; Trevathan-Tackett et al., 2019). These studies have highlighted dynamic microbial responses to environmental variables that have been implicated in acclimatization of the host to abiotic stressors, either through changes in the abundance of bacteria or by colonization of beneficial bacteria (Reshef et al., 2006; Voolstra & Ziegler, 2020). Given the importance of the microbiome and the fundamental role it plays in overall holobiont function (Bordenstein & Theis, 2015; Pita et al., 2018), understanding the factors that drive microbial change is crucial. This is especially true at a time in which historically rapid climate change is occurring (Konopka, 2009).

Sea surface temperatures are predicted to increase 1–3°C by 2100 (Collins et al., 2013), representing a significant challenge to marine organisms. Research has unequivocally shown that many marine species respond to increases in temperature through altered physiological functioning (Shama et al., 2016), behavioral variation (D'Agostino et al., 2020; Shraim et al., 2017), disease susceptibility (Howells et al., 2020), and genomic and epigenomic modifications (Liew et al., 2020; Popovic & Riginos, 2020). There are, however, fewer studies characterizing holobiont-associated microbial dynamics in response to elevated temperatures. To date, studies have shown that temperature influences microbial composition in corals (Wang et al., 2018; Ziegler et al., 2017), sponges (Erwin et al., 2012; Vargas et al., 2020), oysters (Lokmer & Wegner, 2015), anemones (Mortzfeld et al., 2016), and mussels (Li et al., 2019), among others (Brothers et al., 2018). These studies typically focus on a single time-point across a geographic range or temporal variability at a single site (Li et al., 2018; Ward et al., 2017; Woo et al., 2017); rarely are these approaches combined. Further, as almost every step from sample collection to data analysis has been shown to introduce bias, assessing consistent trends using data from many studies that were not processed in the same manner is inherently unreliable (Pollock et al., 2018). Using an approach that includes multiple datasets processed using the same methodology would facilitate a robust characterization of how environmental variables drive microbial dynamics and elucidate conserved microbial responses to temperature.

To this end, we generated two independent datasets investigating the relationship between temperature and the gut microbiota of the sea urchin *Echinometra* sp. EZ. We sampled the gut microbiota because it is integrated with host metabolic and immune systems and is a key regulator of host physiology (Sepulveda & Moeller, 2020). *E. sp. EZ* are found along an extreme environmental gradient between the Persian/Arabian Gulf (herein the PAG) and the Gulf of Oman (herein the GO) which represents an informative system to understand how environmental variables impact the microbiome (Burt et al., 2020). *E. sp. EZ* is the most abundant sea urchin in the PAG (densities average 8.6 m<sup>-2</sup> across eight sites; Burt JA, unpublished data) and they play a significant role in the health and dynamics of coral ecosystems in the region as major bioeroders (Downing & El-Zahr, 1987). The PAG experiences daily mean summer temperatures regularly >35°C and extremes exceeding 37°C (Burt et al., 2019; Smith et al., 2017)

while temperatures in the GO are more typical of oceanic conditions (<32°C in the summer, S. L. Coles (2003)). For our first dataset, we sampled in August and February from six reefs located in the PAG and GO. For the second dataset, we sampled from one reef in the PAG across eight months. We describe community-level differentiation across spatial and temporal gradients, test the hypothesis that rising temperatures result in increased community dispersion, and explore the dynamics between temperature and key microbial taxa.

## 2 | MATERIALS AND METHODS

### 2.1 | Sample collection

Two sampling strategies were implemented in this study, each generating an independent dataset. First, adult *Echinometra* sp. EZ (Ketchum, DeBiasse et al., 2018) were sampled in August 2017 and February 2018 from six sites along the Arabian Peninsula (Table S1, Supporting Information) for a total of 183 samples (Figure 1). This dataset is referred to as the “summer-winter spatial series.” Second, *E. sp. EZ* adults were sampled approximately every other month from March 2017 to February 2018 (Figure S1, Supporting Information) from Saadiyat reef in the PAG, for a total of 120 samples. This dataset is referred to as the “temporal series.” For both sampling strategies we collected 15–17 individuals at each site and/or time point and placed urchins into a 100 L cooler filled with seawater until tissue extractions were performed (within 0–2 h). All of the collection sites are shallow (<7 m) and there are no known thermoclines. The water column is well mixed and a previous study has shown that the difference between bottom temperature and surface temperature is only 0.2°C in the summer (Paparella et al., 2019). Urchins were cut in half with sterile scissors and a fragment of intestine closest to the anus, and its contents, were removed with sterile forceps and placed in RNAlater (Ambion). Tubes were then stored in -20°C after one hour to allow the RNAlater to infiltrate the tissue.

### 2.2 | Environmental variables

The summer-winter spatial series involved six sites along the Arabian Peninsula. We used NOAA's Environmental Research Division Data Access Program (ERDDAP) website to collect sea surface temperature data. The temperature data was downloaded using a bounding box that covered the study area on the day of collection at 12:00:00 UTC (temperature was averaged over one day). In addition, a temperature logger (Onset Hobo Tidbit V2) was deployed on the reef substrate at Saadiyat reef which recorded at 60-minute intervals for the temporal series (Figure S1, Supporting Information). To check the accuracy of the data collected from ERDDAP, a Pearson correlation was used to test for a significant correlation between temperature collected using the two different approaches (Figure S2, Supporting Information). Chlorophyll concentrations were obtained from MODIS AQUA (<https://oceancolor.gsfc.nasa.gov>) level 3 monthly

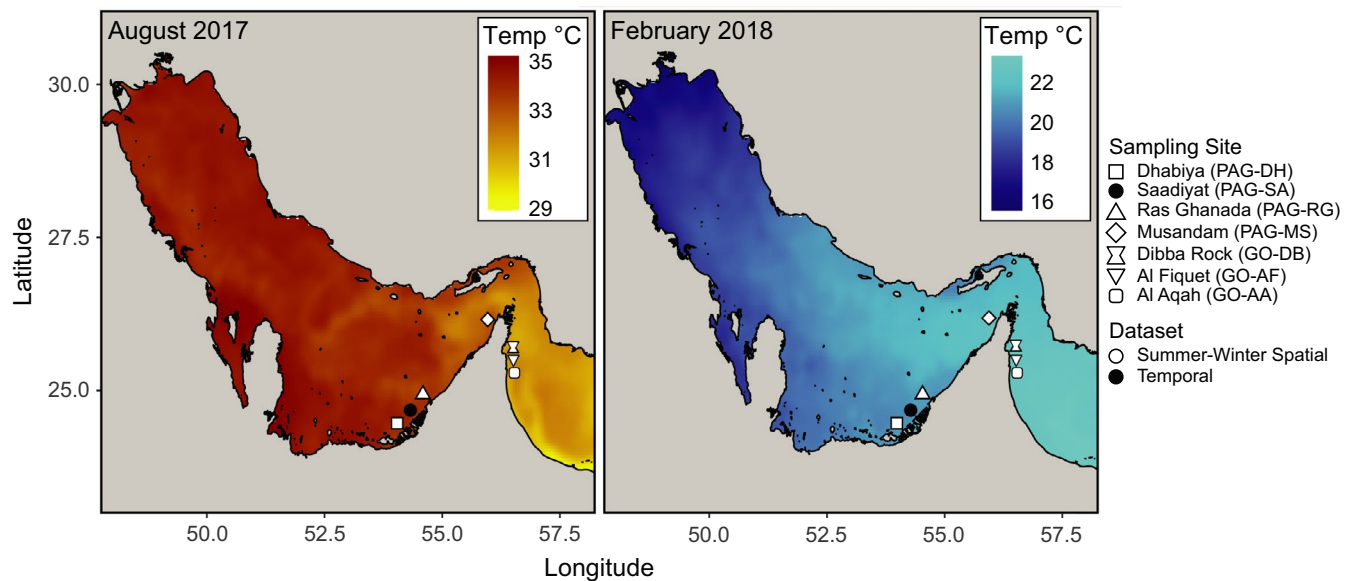


**FIGURE 1** Sampling map of all collection sites in August 2017 and February 2018. The six sampling sites for the summer-winter spatial series are shown in white and the one sampling site for the temporal series is shown in black. Temperature data was downloaded from NOAA's Environmental Research Division Data Access Program (ERDDAP) website (temperatures were averaged over one day and extracted from Aug 15, 2017 and Feb 15, 2018 at 12:00:00 UTC for this plot) [Colour figure can be viewed at [wileyonlinelibrary.com](http://wileyonlinelibrary.com)]

averaged data, and salinity data was obtained from a numeric ocean model: the 1/12 Global Hybrid Coordinate Ocean Model (HYCOM; <https://www.hycom.org/data/glbu0pt08/expt-91pt2>) at 12:00:00 UTC on the day of collections.

### 2.3 | DNA extraction and PCR amplification

Total DNA from urchin guts and their contents was extracted according to the optimized protocol (Method 3) described in Ketchum, Smith, et al., (2018). Briefly, the DNeasy Blood & Tissue Kit (QIAGEN) was used on ~20  $\mu$ L of homogenized sample according to the manufacturers' protocols for extracting animal tissue, with a few modifications. First, we added our sample to 180  $\mu$ L of enzymatic lysis buffer (instead of Buffer ATL); 20 mM TrisCL (pH 8), 2 mM sodium EDTA, 1.2% Triton, 20 mg/ml lysozyme (as described in DNeasy Blood and Tissue Manual). The sample was then incubated for 40 minutes at 37°C. Next, we added 0.5 mL of 0.5 mm zirconia-silica beads (Fisher Scientific) and used a Bead Beater (BioSpec Products) for 40 s at 2,400–3,800 strokes/min and repeated this for a total of three times. Finally, as recommended by the User-Developed Protocol for samples preserved in RNAlater, we used 40  $\mu$ L of proteinase K and 220  $\mu$ L of AL buffer instead of 20 and 200  $\mu$ L, respectively. These additional steps have been shown to more effectively capture traditionally difficult to lyse taxa, such as gram-positive bacteria (Ketchum, et al., 2018).

All samples were then quantified using a Qubit dsDNA High Sensitivity Assay Kit on a Qubit® 2.0 Fluorometer and visualized using a 2% agarose gel. Samples that did not contain sufficient DNA were reextracted and only samples that had a concentration greater than 2 ng/ $\mu$ L were used downstream (n=318). All extraction materials were autoclaved and UV sterilized. DNA extractions and

PCRs were performed in a sterile hood. DNA extractions were normalized to a concentration of 1 ng/ $\mu$ L prior to PCR amplification. PCRs were performed in triplicate 25  $\mu$ L reactions and pooled per individual sample to avoid PCR bias. PCR amplification was performed using the universal V3/V4 PCR primers (forward: 5'-CTACGGGNGGCWGCAG-3'; reverse: 5'-GACTACHVGGGTATCTAATCC-3') (Klindworth et al., 2013) and followed the protocol described in Ketchum, et al., (2018).

To account for potential contamination in the reagents and extraction kits, four blanks were sequenced. One of these blanks was processed through the DNA extraction column with water as the input to identify kit contaminants and three of the blanks were water samples that we ran through PCR and subsequently sequenced.

### 2.4 | Sequencing and sequence data processing

MiSeq indexing adaptors were added following the Illumina 16S Metagenomic Sequencing Library Preparation protocol and an AxyPrep Mag™ PCR Clean-up Kit (Axygen Biosciences, Corning) was used. 16S rRNA gene amplicon libraries were sequenced on the Illumina MiSeq platform using 2 x 300 bp paired-end reads with a 30% PhiX control at the University of North Carolina Charlotte sequencing facility. All 322 (318 microbial samples and four blanks) samples were spread across two sequencing runs with 15 replicate samples on both runs to account for potential run-specific variation. PERMANOVA analyses revealed no significant run-specific effect based on weighted or unweighted unifrac distance ( $R^2 = 0.161766$ ,  $p\text{-value}=0.996$ ,  $R^2 = 0.4529$ ,  $p\text{-value}=0.996$ , respectively).

Raw reads and quality information were imported into QIIME2 v.2020.2 (Bolyen et al., 2019). Each sequencing run was

independently run through DADA2 (Callahan et al., 2016) with a p-trim-left-f of 17 and a p-trim-left-r of 21 to remove adapters/primers, and a quality filter of p-trunc-len-f of 280 and p-trunc-len-r of 220. The two sequencing runs were then combined into one dataset so that it could be filtered and taxonomically annotated more efficiently. The Naïve Bayes classifier was trained on the region of the target sequences and taxonomy was assigned on the combined dataset using Silva 132 reference sequences, clustered at 99% similarity (Quast et al., 2012). As the taxonomical annotation was performed on the combined dataset, there is direct correspondence between ASVs in the spatial and temporal dataset. Sequences matching to Archaea, chloroplast, mitochondria, or sequences that were present in blanks were filtered from the combined dataset. Using the feature-table rarefy command within QIIME2, the dataset was then rarified to 10 400 sequences per sample and samples which had fewer than 10 400 sequences were removed (a total of five samples were removed; A-AF-6, A-DB-6, F-MS-3, A-RG-11, F-MS-19) unless specific downstream software required a nonrarefied dataset. This dataset was subsequently split back into the summer-winter spatial series and the temporal series.

## 2.5 | 16S microbial community analysis

Significant differences in microbial community composition were tested with PERMANOVA using the adonis function in *vegan* v.2.5–6 (Oksanen et al., 2013) on the rarified feature table. The statistical significance of environmental factors (temperature, salinity, and chlorophyll concentration) was analyzed using the function envfit within *vegan* and ordination was performed using NMDS based on Bray-Curtis dissimilarity. Pearson correlation was used to test for significant correlations between temperature and salinity in the two datasets (Figure S3 and S4, Supporting Information). Feature tables were imported into ampvis2 (Andersen et al., 2018) to run Principal Component Analysis (PCA) using Bray-Curtis dissimilarities, a Hellinger transformation, and the “filter\_species” flag set to zero. The temporal series was divided into three groups based on the temperature on the day of collection: summer (33–34°C), intermediate (26–32°C), and winter (20–24°C) to reveal large-scale patterns. We calculated alpha diversity metrics, including the Shannon diversity index and observed features metric, through the QIIME2 core diversity metrics plugin. We then tested for significant differences in alpha diversity indices with a Kruskal-Wallis test and applied the Benjamini-Hochberg false discovery rate correction for multiple comparisons (Thissen et al., 2002).

Next, we tested the hypothesis that thermally stressful conditions may result in an increase in microbial community dispersion as the host becomes less able to regulate their microbiome (in line with the Anna Karenina Principle (Zaneveld et al., 2017)). In the summer-winter spatial series, we hypothesized that dispersion would increase in August compared to February for the PAG sites due to the uncharacteristically hot summer of 2017 (Paparella et al., 2019), which was likely physiologically stressful for urchins. For the temporal series,

we hypothesized that dispersion would increase in summer 2017. To test these hypotheses, analysis of multivariate homogeneity of group dispersion was quantified by conducting permutation tests based on Bray-Curtis dissimilarities and applying Tukey's HSD (PERMDISP2, Anderson et al. (2006)) using the package *vegan* v.2.5–6.

In order to elucidate specific microbial signatures that associate with temperature, we used *selbal* which outperforms other methods commonly used in microbiome research by selecting the smallest number of variables with a higher discrimination accuracy (Susin et al., 2020). Prior to running *selbal*, feature tables were filtered to remove ASVs that were not consistently present in the data (ASVs that were found in less than 20% of samples were removed). The analysis of microbiome communities is challenging due to the compositional aspect of these data, as the relative nature of ASV abundances can lead to spurious correlations. To circumvent these issues, *selbal* uses balances, or relative abundances of two groups of taxa, which preserves the principles of compositional data analysis. *Selbal* uses an algorithm that starts with a scan for two taxa whose balances (or log ratios) most closely associate with the response variable, in this case temperature. Once these two taxa are selected, the algorithm then sequentially adds new taxa to the balance such that the predictive power is improved. This process continues until there are no new variables that can improve the optimization or when the maximum number of components are reached. *Selbal* was run on both independent datasets with an “n.fold” or “number of folds in the cross-validation procedure” of 5, 10 iterations, and the “covar” flag set to NULL (as recommended when working with a continuous variable). For the summer-winter spatial series, the temperature data consisted of the output from the NOAA ERDDAP website. For the temporal series, temperature was derived from the HOBO logger and averaged over the day of sampling. The raw *selbal* output can be found in Figure S5 and S6, Supporting Information. ASVs that *selbal* found to be predictive of temperature were then extracted from the feature tables and their abundances were used to generate bubble plots (Zorz, 2019). We performed a search using the Nucleotide Basic Local Alignment Search Tool (BLASTn) on the ASVs identified by *selbal* against NCBI's Nucleotide collection (nr/nt) database in order to identify ASVs to species level, where possible. An e-value cutoff of  $10^{-8}$  was used and only BLAST hits with 100% identity were retained.

To explore how ASVs that were predictive of temperature from the *selbal* output fit into the context of the wider microbial network, we conducted network analysis using SpiecEasi (Sparse inverse covariance estimation for ecological association inference, Kurtz et al., (2015)) v1.1.1 on the two datasets (Supplemental Methods, Figure S7 and S8, Supporting Information). Further, we used Phylogenetic Investigation of Communities by Reconstruction of Unobserved States (PICRUSt v2.0.0, Douglas et al., (2020)) to characterize microbial pathways enriched during warmer conditions (Supplemental Methods, Figure S9 and S10, Supporting Information).

DEICODE (Martino et al., 2019), a robust Aitchison PCA, was implemented within QIIME2 to identify ASVs responsible for the differences between the PAG and the GO by looking for ASVs

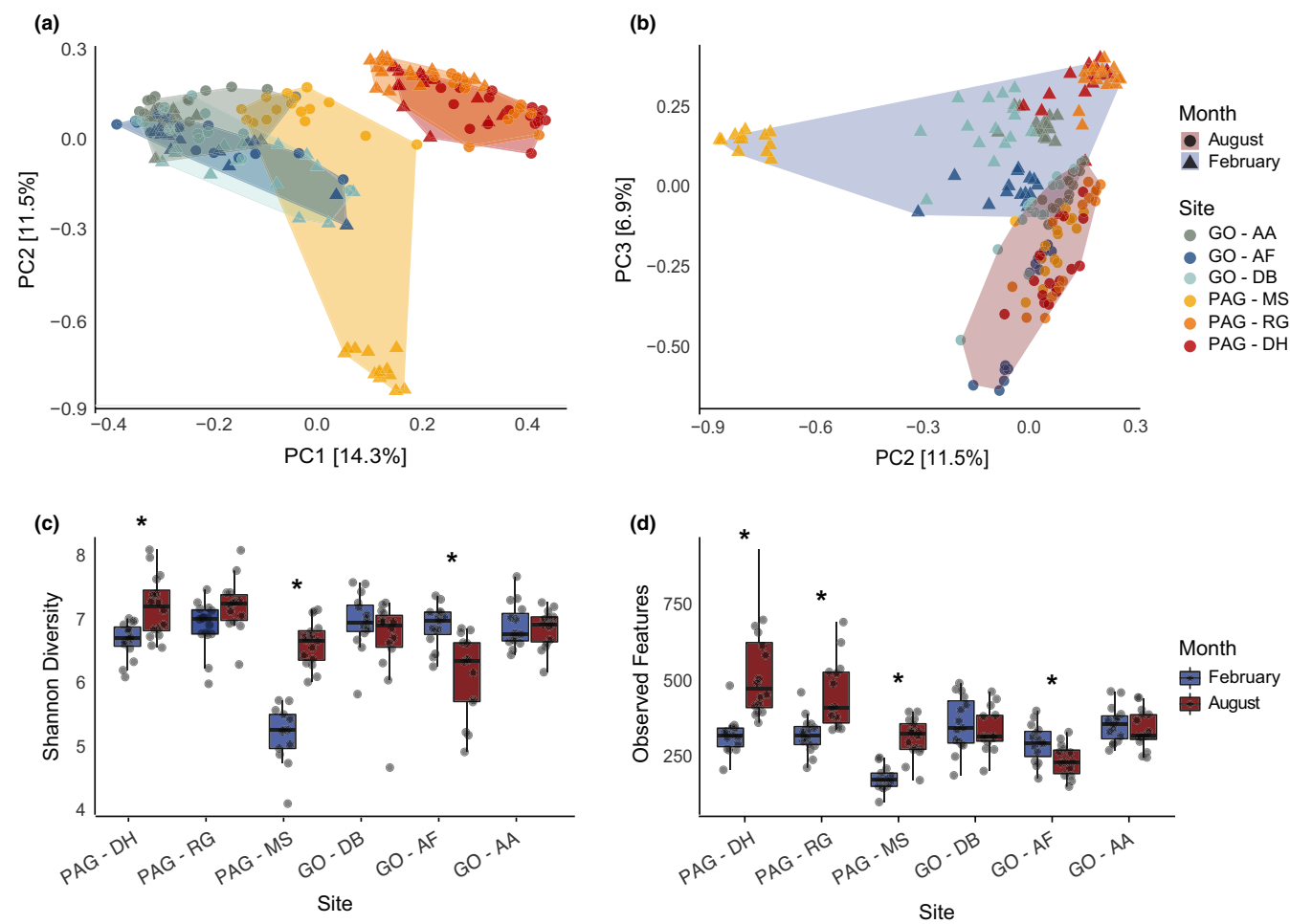


**FIGURE 2** Microbial diversity from the summer-winter spatial series. (a) Principal Component Analysis based on Bray-Curtis dissimilarities after a Hellinger transformation of bacterial communities from three sites within the PAG and three sites within the GO. The shaded color represents collection sites and the shape of the point represents month of collection. (b) PCA showing principal component two and three and shaded according to month of collection. (c) Box plots of Shannon Diversity metrics for all collection sites and split by month of collection. (d) Box plots of observed features for all collection sites and split by month of collection. Asterisks denote significant differences in Shannon Diversity or number of observed features when comparing between month of collection within each site, respectively [Colour figure can be viewed at [wileyonlinelibrary.com](http://wileyonlinelibrary.com)]

which drive the clustering along PC 1. The un rarefied summer-winter spatial series dataset was used with a --p-min-feature-count of 10 and --p-min-sample-count of 500. The ordination file output from DEICODE was then exported and the top ten and bottom ten feature loadings were input into Rstudio and plotted in a heatmap.

Figures were created in R using ggplot2 and illustrations were further stylized in Adobe Illustrator.

### 3 | RESULTS

#### 3.1 | Study Design

Our study design implemented two sampling strategies and resulted in two independent datasets. The summer-winter spatial series consisted of 183 samples collected from six different reefs in both

August and February (Figure 1). This dataset covers an extreme environmental gradient across sites as well as two thermally distinct months; August 2017 (summer) and February 2018 (winter). The temporal series consisted of 120 samples across eight months from one sampling site (PAG-SA; Figure 1) with large seasonal temperature variation (~17°C).

#### 3.2 | Differences in microbiota composition and diversity in the summer-winter spatial series

The summer-winter spatial series showed differences in overall microbiota composition, as measured by Bray-Curtis dissimilarities. There was clear differentiation between the PAG and the GO along PC 1 with PAG-MS samples clustered between samples collected from the two seas (Figure 2A). Samples collected from PAG-MS in February were differentiated from the rest of the dataset along PC

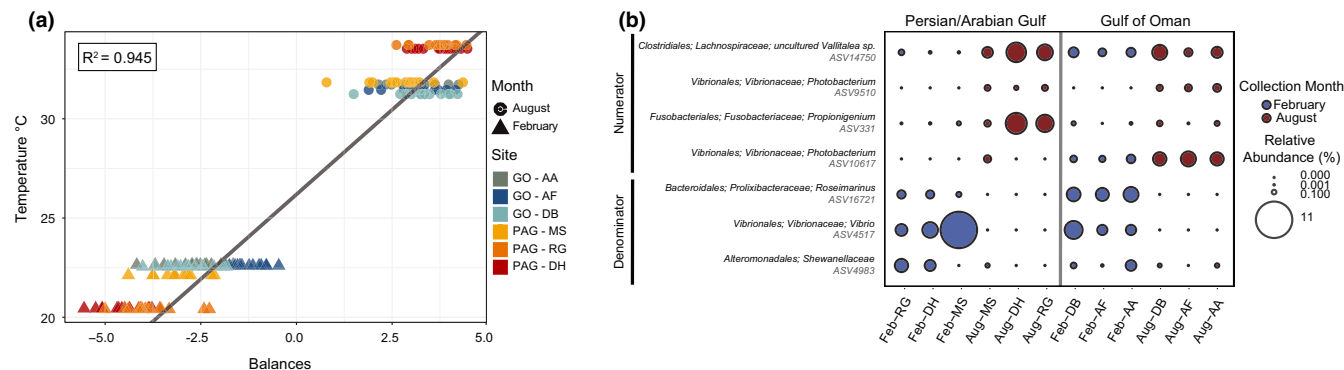


**FIGURE 3** (a) Regression model of the seven variables that define the balance for the summer-winter spatial series. The shape of the points represents month of collection and color represents the site where the samples were collected. (b) The variables that define the balance are taxonomically annotated in the bubble plot and their position in the balance is labelled “Numerator” or “Denominator.” The size of the bubble corresponds to the relative abundance in the count table and the color of the bubble represents the month the samples were collected [Colour figure can be viewed at [wileyonlinelibrary.com](http://wileyonlinelibrary.com)]

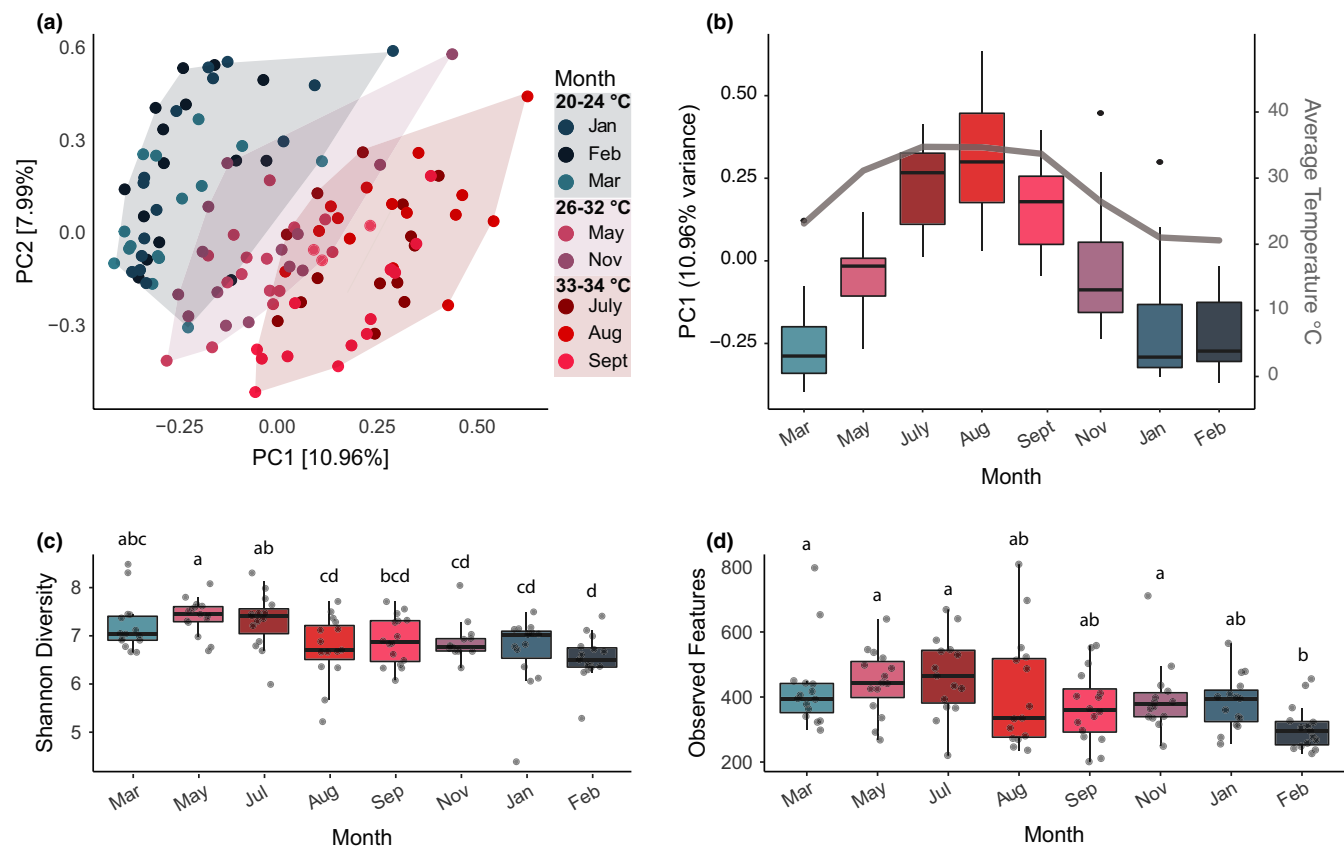


**FIGURE 4** Microbial diversity of the temporal series. (a) PCA based on Bray-Curtis dissimilarities after a Hellinger transformation of bacterial communities across eight months from Saadiyat reef, in the PAG. The color of the point represents collection month and the shaded regions represent the temperatures at the time of collection. (b) The eigenvalues from the first principal component were extracted and plotted alongside the average temperature on the day of collection. (c) Box plots of Shannon Diversity metrics for all collection months. (d) Box plots of observed features for all collection months. For plots C and D, boxes that do not share similar letters denote statistical significance ( $p < 0.05$ , Kruskal-Wallis test with a Benjamini & Hochberg correction) [Colour figure can be viewed at [wileyonlinelibrary.com](http://wileyonlinelibrary.com)]

2. Samples collected in August were differentiated from those collected in February along PC 3 (Figure 2B). PERMANOVA analyses showed a significant effect of gulf ( $R^2 = 0.1335$ ,  $p$ -value < 0.001), site ( $R^2 = 0.1757$ ,  $p$ -value < 0.001), month ( $R^2 = 0.0634$ ,  $p$ -value < 0.001), gulf by month ( $R^2 = 0.0367$ ,  $p$ -value < 0.001), and site by month ( $R^2$

= 0.1134,  $p$ -value < 0.001) on community composition (Table S2, Supporting Information). Envfit analysis showed a significant correlation between NMDS ordination of the microbial community structure and temperature ( $R^2 = 0.1850$ ,  $p$ -value < 0.003), chlorophyll concentration ( $R^2 = 0.4581$ ,  $p$ -value < 0.003), and salinity ( $R^2$

0.5185,  $p$ -value <0.003, Table S3 and S4, Supporting Information). The NMDS ordination plot showed that these three environmental variable vectors were orthogonal to one another (Figure S11, Supporting Information). We used DEICODE to identify the main taxa driving the differences along PC 1 (i.e., between the two seas). We found that ASVs classified as *Spirochaeta* (ASV8874), *Desulfotalea* (ASV14864), *Bacteroidia* (ASV11638 and ASV13084), *Roseimarinus* (ASV5463), and *Marinifilaceae* (ASV4027) were more abundant in the GO and two different *Vibrio* taxa (ASV12189 and ASV1103), *Propionigenium* (ASV331), and *Photobacterium* (ASV16623) were more abundant in the PAG (Figure S12, Supporting Information).

There were significant differences in the Shannon Diversity Index (Figure 2C) when comparing August to February for PAG-DH, PAG-MS, and GO-AF. For the number of observed features (or ASVs, Figure 2D), there were significant differences between PAG-DH, PAG-MS, PAG-RG and GO-AF ( $p$ -value <0.05, Kruskal-Wallis; see Table S5, Supporting Information for all pairwise comparisons). Notably, diversity metrics were higher in August than February for all of the PAG sites and, inversely, lower in August than February for all of the GO sites. Permutation tests of multivariate dispersion showed that dispersion was significantly higher in August than February in PAG-MS (Figure S13 and Table S6, Supporting Information).

### 3.3 | Specific ASVs correlate with increasing temperature across a wide geographic range and between summer and winter

In the *selbal* analysis, we identified ASVs that were associated with temperature between collection months at each site in the summer-winter spatial series. The numerator and denominator in the *selbal* output contains taxa whose relative abundances increase and decrease, respectively, with increasing temperatures. *Selbal* analysis determined that the optimal number of variables was seven. With these seven ASVs, we obtained a  $R^2$  value of 0.945 for the regression model (Figure 3A). The relative abundance of four of the seven ASVs increased with increasing temperatures (uncultured *Vallitalea* sp. [ASV14750], *Propionigenium* sp. [ASV331], and two *Photobacterium* sp. [ASV9510 and ASV10617], see Figure 3B) and three of the ASVs decreased with increasing temperature (*Roseimarinus* sp. [ASV16721], *Vibrio* sp. [ASV4517], and *Shewanellaceae* sp. [ASV4983]).

### 3.4 | Differences in microbiota composition and diversity in the temporal series

The temporal series showed differences in overall microbiota composition, as measured by Bray-Curtis dissimilarities (Figure 4A). There was clear differentiation on PC 1 between samples grouped by temperature at the time of collection. The major axis of community variation (eigenvalues from PC 1, Figure 4B) was significantly correlated with the average temperature on the day of collection ( $R = 0.76$ ,  $p$ -value <2.2e-16; Figure S14, Supporting Information).

PERMANOVA analysis showed a significant effect of season (summer, winter, and intermediate;  $R^2 = 0.12272$ ,  $p$ -value <0.001) and month ( $R^2 = 0.13967$ ,  $p$ -value <0.001) on community composition (Table S7, Supporting Information). Envfit analysis showed a significant correlation between NMDS ordination of the microbial community structure and temperature ( $R^2 = 0.7124$ ,  $p$ -value <0.003), with weaker correlations with chlorophyll concentration ( $R^2 = 0.1951$ ,  $p$ -value <0.003), and salinity ( $R^2 = 0.1732$ ,  $p$ -value <0.003, Table S8 and S9, Supporting Information). The NMDS ordination plot showed that the salinity vector was orthogonal to the temperature and chlorophyll vectors which were overlapping (Figure S15, Supporting Information). There were significant differences between specific months for both Shannon Diversity Indices (Figure 4C) and observed features (Figure 4D, Table S10, Supporting Information). For the Shannon Diversity Index, February was significantly lower than March, May, and July and January was significantly lower than May and July. Further, July is significantly higher than November, August is significantly lower than July and May, and May is significantly higher than both November and September. For observed features, February was significantly lower than March, May, July, and November. No significant differences in alpha diversity metrics were found when comparing between the three different temperature groups after a Benjamini & Hochberg correction (Table S10, Supporting Information). Permutation tests of multivariate dispersion analyses revealed that dispersion was significantly higher in August compared to all other months except for March (Figure S16, Supporting Information). No significant differences occurred between the other months (Table S6, Supporting Information).

### 3.5 | Specific ASVs correlate with increasing temperature in a sampling dataset with high temporal resolution

The *selbal* analysis identified ASVs that were associated with temperature between collection months in our temporal series. *Selbal* identified that the optimal number of variables was eight and these eight ASVs resulted in a  $R^2$  value of 0.966 for the regression model (Figure 5A). The relative abundance of four of the ASVs increased as temperature rose (*Propionigenium* sp. [ASV331], uncultured *Vallitalea* sp. [ASV14750], and 2 ASVs belonged to *Vibrio* [ASV12030 and ASV1103], see Figure 5B) and the relative abundance of the other four ASVs decreased (two *Vibrio* spp. [ASV679 and ASV4517], *Roseimarinus* sp. [ASV5483], and *Photobacterium* sp. [ASV4592]). While there were several ASVs which were taxonomically labelled as *Vibrio* spp., they all represent unique sequence variants.

### 3.6 | Consistent responses to temperature in both independent datasets

Three identical ASVs were identified as correlating with temperature in the two independent *selbal* analyses (these are denoted in

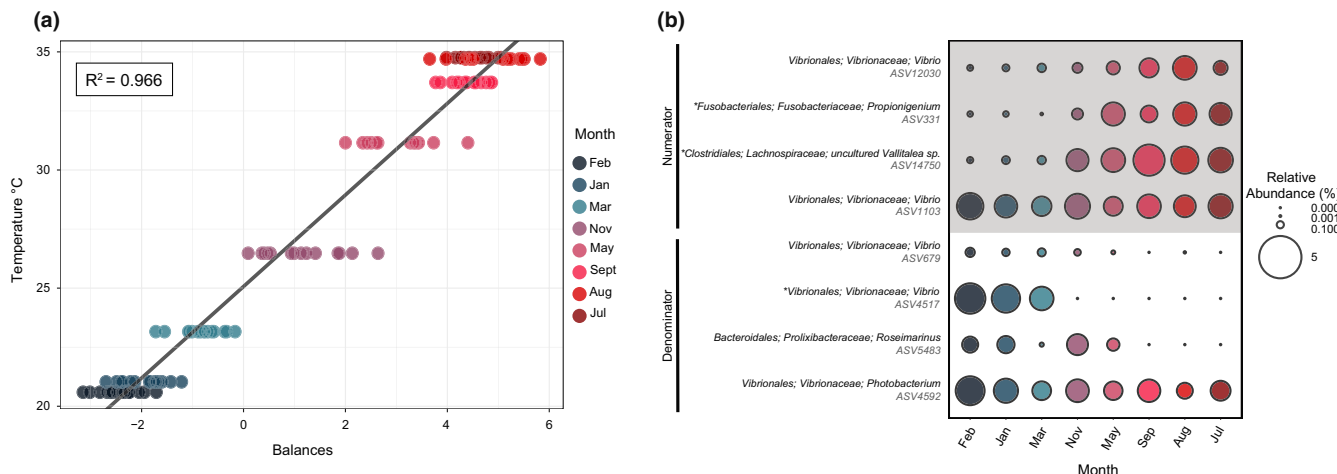


**FIGURE 5** (a) Regression model of the eight variables that define the balance for the temporal series. The color of the points represents the month at which they were collected. (b) The variables that define the balance are taxonomically annotated in the bubble plot and their position in the balance is labelled “Numerator” or “Denominator.” The size of the bubble corresponds to relative abundance in the count table and the color of the bubble represents month of collection. ASVs which were retained from both datasets in *selbal* analysis are denoted by an asterisk [Colour figure can be viewed at [wileyonlinelibrary.com](http://wileyonlinelibrary.com)]

Figure 5B by an asterisk in front of the taxonomic ID). These three ASVs were *Propionigenium* sp. (ASV331), uncultured *Vallitalea* sp. (ASV14750), and *Vibrio* sp. (ASV4517). The *Vibrio* sp. strain was further classified through a BLAST search as *Vibrio chagasici* (100% identity score, expect value 0.0, accession number: MT269630.1). *V. chagasici* became relatively less abundant as temperature increased. We were unable to confidently classify any additional ASVs to the species level. Beyond these specific ASVs, there was also taxonomic redundancy in the two analyses. Although ASV identifiers were different, strains of both *Roseimarinus* spp. and *Photobacterium* spp. were identified in both *selbal* analyses. However, while the abundance trend for *Roseimarinus* spp. was consistent across datasets, *Photobacterium* spp. was identified as a numerator in the summer-winter spatial series and as a denominator in the temporal series.

SpiecEasi network analyses retained all of the ASVs output by *selbal*. The *selbal* ASVs did not consistently co-occur with each other in either of the two datasets. Further, they were not identified as keystone microbes based on their hubbiness (Figure S7 and S8, Supporting Information). PICRUSt2 analyses showed that both datasets were enriched for pathways related to cell wall machinery in the warmer sampling months. Further, both datasets showed an enrichment in sucrose biosynthesis and degradation-related pathways for samples collected in the cooler months (Figure S9 and S10, Supporting Information).

## 4 | DISCUSSION

All multicellular organisms associate with a diverse microbiome that contributes to the physiology, development, and fitness of their host (Voolstra & Ziegler, 2020). A fundamental question in animal-microbe interactions is how the structure and function of the microbiome is

influenced by environmental variables and which variables are the main drivers of microbial variation. It is particularly important to understand temperature-related microbial dynamics as historically rapid climate change is occurring. While assessing community-level changes across environmental gradients is informative, extracting specific microbial taxa that correlate with environmental variables is crucial for building predictive models for diagnosis of, for example, dysbiosis, stress responses, or disease states (Rivera-Pinto et al., 2018). To this end, we generated two independent datasets that spanned an extreme thermal gradient with high temporal resolution in order to assess both community-level changes, as well as highlight temperature-predictive microbial taxa.

In the summer-winter spatial series, the majority of the variation in the data was explained by collection site where PC 1 differentiated the PAG from the GO. This microbial differentiation was congruent with previous analyses on the genetic structure of the host species, which showed two populations, one in the PAG and one in the GO (Ketchum et al., 2020). The Musandam collection site is located within the Strait of Hormuz and is geographically situated at the connection between the two seas. The intermediate geographic location is mirrored in the PCA where the samples from Musandam are located between samples from the PAG and GO on PC 1. Additionally, this site is thermally divergent from the two seas so it is unclear whether this differentiation on PC 1 is a result of geographic location or environmental conditions. Differences in microbiota composition were also identified according to the month of sampling. This variation is likely due to seasonal temperature changes of about 20°C in the PAG (S. L. Coles, 2003) and 10°C in the GO (S. Coles, 1997). While there is differentiation in the ordination data which correlates with salinity and chlorophyll concentration, these variables do not follow the same pattern as temperature and their ordination vectors are orthogonal to each other. This makes it unlikely that salinity and chlorophyll concentration are responsible

for the differentiation between August and February. It is also possible that this differentiation is a result of shifting dietary patterns, although this would likely correlate with chlorophyll concentrations and therefore would have been identified in our analysis. Interestingly, measures of microbial diversity were higher and generally more variable in August than February for all PAG sites but in the GO sites this pattern was not evident. This increase in alpha diversity in the PAG may be an adaptive mechanism which allows the urchins to meet their energy and nutrient demands during warmer months or could simply be a result of optimal growth temperatures for a wider variety of microbiota. In our temporal series, we saw a similar pattern in which temperature was a likely driver of community composition; samples clustered by the temperature at which they were collected and we found a significant correlation between temperature and community composition. While other factors like salinity and chlorophyll concentration may contribute to this differentiation (ordination vectors between temperature and chlorophyll concentration were overlapping and temperature and salinity were weakly correlated), temperature was the single most contributing factor with respect to community composition and ordination. Our alpha diversity analysis revealed a temporal oscillation where diversity was generally higher in warmer months, however this relationship was not always significant. Overall, temperature was a robust predictor of community-level variation in both independent datasets.

With both datasets, we tested for the Anna Karenina Principle (AKP) (Zaneveld et al., 2017) which states that stressed organisms may host more stochastic microbiomes than healthy organisms due to the host being unable to regulate their microbiome. In the summer of 2017, there was a mass coral bleaching event that occurred between July and August in the southern PAG and reef-bottom temperatures were among the hottest on record with benthic organisms spending about two months at temperatures exceeding 34°C (Burt et al., 2019). Therefore, for the summer-winter spatial series, we hypothesized that the 2017 coral bleaching event would be physiologically stressful for urchins and would result in an increase in microbial dispersion in August compared to February. Similarly, we hypothesized that July and August would be physiologically stressful and would result in an increase in dispersion in the temporal series. For the summer-winter spatial series we only found evidence for a significant increase in dispersion in Musandam between August and February. For the temporal series, we found that August was significantly more disperse than all of the other months except for March. It is unclear why the summer-winter spatial series did not highlight an increase in dispersion in August for the southern PAG sites while the temporal series did. It is possible that the differences in dispersion for the southern PAG sites were swamped by the difference between August and February for Musandam (dispersion was higher in August for all sites, although not significant). There may also be a different abiotic stressor which we have not measured that is only affected the Musandam population (e.g., runoff, sewage, or industrial waste). Alternatively, Dhabiya and Ras Ghanada may have been more protected from thermal extremes than Saadiyat. However, this pattern was not evident in Burt et al., (2019), where temperatures

on Saadiyat reef paralleled those from Dhabiya and Ras Ghanada. With the increased resolution in the temporal dataset, we were able to show that dispersion was highest during the peak of the coral bleaching event. However, it is unclear why dispersion in March was also quite high. There may be another stressor affecting dispersion in March that is unaccounted for. Finally, we did not observe an increase in dispersion in July when temperatures began to steadily increase. It is possible that we collected urchins in July before they became physiologically stressed or that there is a time-lag between temperature change and microbial shifts. Here we provide some evidence for the AKP, however, future work is needed to ascertain at what temperature *E. sp. EZ* becomes physiologically compromised to better understand the relationship between dispersion and thermal stress in sea urchins.

In order to go beyond community-level descriptions, we used *selbal* to identify key microbial signatures whose balances were predictive of temperature. We performed this analysis on both independent datasets and found striking patterns. In addition to the taxonomic redundancy in the ASVs that were identified, three ASVs were identified by *selbal* in both datasets. The consistency of these ASV trends across the two datasets were also reflected in the putative functional profiles associated with temperature. The presence of the same ASVs across datasets may point to a consistent microbial biomarker that is responsible for the maintenance of host homeostasis or is opportunistically proliferating (and may be pathogenic) in response to temperature change.

Over 50% of the ASVs identified from the two *selbal* analyses were strains of Vibrionaceae, highlighting a consistent temperature-dependent response from this family of Proteobacteria. Vibrios, as well as *Photobacterium* spp. (which belongs to the Vibrionaceae family), are found in aquatic habitats throughout the world and occupy a wide variety of ecological niches, sometimes as beneficial symbionts (McFall-Ngai & Ruby, 1991; Thompson et al., 2004) or as potential pathogens (Cervino et al., 2008; Fabbro et al., 2012; Newton et al., 2012). Species in these taxonomic groups have been observed in several species of sea urchins (Beleneva & Kukhlevskii, 2010; Hakim et al., 2016; Yao et al., 2019) and their abundance has been shown to increase in response to temperature in the coral *Pocillopora damicornis* (Tout et al., 2015). We did not see a pattern in which increased temperatures consistently resulted in an increase in Vibrionaceae strains, rather we found that some strains increased and some decreased in relative abundance. Together, these results point to an interesting relationship between Vibrionaceae spp. and temperature that warrants further investigation due to the great variability in phenotypic and pathogenic profiles within this family.

Two other ASVs were identified in both datasets as predictive of temperature and were taxonomically labelled as an uncultured strain of *Vallitalea* sp. (from the Lachnospiraceae family) and *Propionigerium* sp., both of which increase in relative abundance when temperature increases. Additionally, *Roseimarinus* spp. were identified in both analyses, although the ASVs differed. *Vallitalea* is a relatively poorly described genus with only three species described to date. These species were isolated from hydrothermal systems (Aissa et al., 2014; Schouw et al., 2018; Sun et al., 2019),

which may indicate extreme thermal tolerance. *Vallitalea guaymasensis* has been classified as a bacterial indicator species associated with the coral *Porites lutea* from the Gulf of Thailand and Andaman Sea (Pootakham et al., 2017). However, a study on the conspecific *P. lobata* from the PAG and GO did not find *V. guaymasensis* in their microbiome data (Hadaidi et al., 2017). *Propionigenium* has been identified as one of the most abundant bacterial taxa in the guts of five different sea urchins (Yao et al., 2019) and is likely involved in the metabolism of carbohydrates, amino acids, and lipids (Hakim et al., 2016). *Propionigenium* has also been shown to be involved in a variety of different host health benefits, not limited to sea urchins. For example, it has been associated with the modulation of the lifespan of the killifish *Nothobranchius furzeri* (Smith, Willemsen, et al., 2017). Unlike *Vallitalea* sp. and *Propionigenium* sp., *Roseimarinus*' abundance decreases as temperature increases. Although the exact biological function that *Roseimarinus* spp. play in their host is unknown, it has been isolated in other marine microbial studies and has been shown to decrease in relative abundance as temperature increases in the mussel *Mytilus galloprovincialis* (Li et al., 2019). Although beyond the scope of this study, it would be beneficial to determine whether these changes in microbial abundances are a direct consequence of temperature change on the microbes (i.e., changes in relative abundance of microbes across season or site is simply due to different optimal growth temperatures) or indirect selection of microbial abundance by the host requiring different microbes in response to changing metabolic needs.

Assessing how environmental variables drive microbial diversity underpins our understanding of the relationships between hosts and their microbiome. Our sampling strategy has allowed us to characterize the microbial gut community across a wide geographic and temporal span and implicate temperature as a regulator of community composition. We take this further by identifying bacterial taxa whose abundances correlate with temperature and find a consistent signature response in the two independent datasets. As the PAG is the warmest sea in the world, it is a highly informative model for our understanding of the microbial response to thermal extremes as well as for predicting microbial shifts in response to climate change. The observed patterns presented in this study align well with the idea that acclimatization through restructuring of the microbial community constitutes a dynamic environmental response mechanism. We identified several key microbial taxa that may either represent opportunistic pathogens or be crucial for the maintenance of host homeostasis during thermal extremes.

## ACKNOWLEDGEMENTS

This work was supported by NSF Award 1924498 to AMR and JAB; incentive funds from UNC Charlotte to AMR; a NSF Graduate Research Fellowship (GRF) to RNK; the NYUAD Water Research Center grant CG007 to JAB; and the International Coral Reef Society (ICRS) Graduate Fellowship to RNK. The field work was carried out using the Marine Biology Core Technology Platform resources at New York University Abu Dhabi, and this support is greatly appreciated. We thank the Environmental Agency – Abu Dhabi for permits.

## CONFLICT OF INTEREST

The authors declare that they have no conflict of interest.

## AUTHOR CONTRIBUTIONS

RNK designed and performed research, analyzed data, and wrote the manuscript. EGS performed research, analyzed data, and helped with urchin collections. GOV, DM, and NAM helped with urchin collections. JAB contributed lab space and collection assistance. AMR helped with data analysis, writing the manuscript, and contributed sequencing funds. All authors contributed to the final paper.

## DATA AVAILABILITY STATEMENT

Sequence data, metadata, and count tables are available on Dryad (<https://doi.org/10.5061/dryad.r7sqv9sb1>), as well as on the Biological & Chemical Oceanography Data Management Office website under Project Number 817793.

## ORCID

Remi N. Ketchum  <https://orcid.org/0000-0002-0818-2908>  
 Edward G. Smith  <https://orcid.org/0000-0003-0842-7757>  
 John A. Burt  <https://orcid.org/0000-0001-6087-6424>  
 Adam M. Reitzel  <https://orcid.org/0000-0001-5734-7118>

## REFERENCES

Aissa, F. B., Postec, A., Erauso, G., Payri, C., Pelletier, B., Hamdi, M., & Fardeau, M.-L. (2014). *Vallitalea pronyensis* sp. nov., isolated from a marine alkaline hydrothermal chimney. *International Journal of Systematic and Evolutionary Microbiology*, 64(4), 1160–1165.

Andersen, K. S., Kirkegaard, R. H., Karst, S. M., & Albertsen, M. (2018). Ampvis2: an R Package to Analyse and Visualise 16S rRNA Amplicon Data. *bioRxiv*, 299537.

Anderson, M. J., Ellingsen, K. E., & McArdle, B. H. (2006). Multivariate dispersion as a measure of beta diversity. *Ecology Letters*, 9(6), 683–693. <https://doi.org/10.1111/j.1461-0248.2006.00926.x>

Bayer, K., Schmitt, S., & Hentschel, U. (2008). Physiology, phylogeny and in situ evidence for bacterial and archaeal nitrifiers in the marine sponge *Aplysina aerophoba*. *Environmental Microbiology*, 10(11), 2942–2955.

Beleneva, I., & Kukhlevskii, A. (2010). Characterization of *Vibrio gigantis* and *Vibrio pomeroyi* isolated from invertebrates of Peter the Great Bay Sea of Japan. *Microbiology*, 79(3), 402–407. <https://doi.org/10.1134/S0026261710030173>

Bolyen, E., Rideout, J. R., Dillon, M. R., Bokulich, N. A., Abnet, C. C., Al-Ghalith, G. A., Alexander, H., Alm, E. J., Arumugam, M., Asnicar, F., Bai, Y., Bisanz, J. E., Bittinger, K., Brejnrod, A., Brislawn, C. J., Brown, C. T., Callahan, B. J., Caraballo-Rodríguez, A. M., Chase, J., ... Caporaso, J. G. (2019). Reproducible, interactive, scalable and extensible microbiome data science using QIIME 2. *Nature Biotechnology*, 37(8), 852–857. <https://doi.org/10.1038/s41587-019-0209-9>

Bordenstein, S. R., & Theis, K. R. (2015). Host biology in light of the microbiome: ten principles of holobionts and hologenomes. *PLOS Biology*, 13(8), e1002226. <https://doi.org/10.1371/journal.pbio.1002226>

Brothers, C. J., Van Der Pol, W. J., Morrow, C. D., Hakim, J. A., Koo, H., & McClintock, J. B. (2018). Ocean warming alters predicted microbiome functionality in a common sea urchin. *Proceedings of the Royal Society B*, 285(1881), 20180340. <https://doi.org/10.1098/rspb.2018.0340>

Burt, J. A., Camp, E. F., Enochs, I. C., Johansen, J. L., Morgan, K. M., Rieg, B., Hoey, A. S. (2020). Insights from extreme coral reefs in a changing world. *Coral Reefs*, 39(3), 495–507. <http://dx.doi.org/10.1007/s00338-020-01966-y>

Burt, J. A., Paparella, F., Al-Mansoori, N., Al-Mansoori, A., & Al-Jailani, H. (2019). Causes and consequences of the 2017 coral bleaching event in the southern Persian/Arabian Gulf. *Coral Reefs*, 38(4), 567–589. <https://doi.org/10.1007/s00338-019-01767-y>

Callahan, B. J., McMurdie, P. J., Rosen, M. J., Han, A. W., Johnson, A. J. A., & Holmes, S. P. (2016). DADA2: high-resolution sample inference from Illumina amplicon data. *Nature Methods*, 13(7), 581. <https://doi.org/10.1038/nmeth.3869>

Carrier, T. J., Lessios, H. A., & Reitzel, A. M. (2020). Eggs of echinoids separated by the Isthmus of Panama harbor divergent microbiota. *Marine Ecology Progress Series*, 648, 169–177. <https://doi.org/10.3354/meps13424>

Cervino, J., Thompson, F., Gomez-Gil, B., Lorence, E., Goreau, T., Hayes, R., & Bartels, E. (2008). The *Vibrio* core group induces yellow band disease in Caribbean and Indo-Pacific reef-building corals. *Journal of Applied Microbiology*, 105(5), 1658–1671.

Coles, S. (1997). Reef corals occurring in a highly fluctuating temperature environment at Fahal Island, Gulf of Oman (Indian Ocean). *Coral Reefs*, 16(4), 269–272. <https://doi.org/10.1007/s003380050084>

Coles, S. L. (2003). Coral species diversity and environmental factors in the Arabian Gulf and the Gulf of Oman: a comparison to the Indo-Pacific region. *Atoll Research Bulletin*. <https://doi.org/10.5479/si.00775630.507.1>

Collins, M., Qin, D., Stocker, T. F., Plattner, G.-K., Tignor, M., Allen, S. K., & Midgley, P. M. (2013). In *Climate Change 2013: The Physical Science Basis. Contribution of Working Group I to the Fifth Assessment Report of the Intergovernmental Panel on Climate Change*. Cambridge University Press. 1029–1136.

D'Agostino, D., Burt, J. A., Reader, T., Vaughan, G. O., Chapman, B. B., Santinelli, V., Cavalcante, G. H., & Feary, D. A. (2020). The influence of thermal extremes on coral reef fish behaviour in the Arabian/Persian Gulf. *Coral Reefs*, 39(3), 733–744. <https://doi.org/10.1007/s00338-019-01847-z>

Douglas, G. M., Maffei, V. J., Zaneveld, J. R., Yurgel, S. N., Brown, J. R., Taylor, C. M., Huttenthaler, C., & Langille, M. G. I. (2020). PICRUSt2 for prediction of metagenome functions. *Nature Biotechnology*, 38(6), 685–688. <https://doi.org/10.1038/s41587-020-0548-6>

Downing, N., & El-Zahr, C. (1987). Gut evacuation and filling rates in the rock-boring sea urchin, *Echinometra mathaei*. *Bulletin of Marine Science*, 41(2), 579–584.

Erwin, P. M., Pita, L., López-Legentil, S., & Turon, X. (2012). Stability of sponge-associated bacteria over large seasonal shifts in temperature and irradiance. *Applied and Environmental Microbiology*, 78(20), 7358–7368. <https://doi.org/10.1128/AEM.02035-12>

Fabbro, C., Celussi, M., Russell, H., & Del Negro, P. (2012). Phenotypic and genetic diversity of coexisting *Listonella anguillarum*, *Vibrio harveyi* and *Vibrio chagassi* recovered from skin haemorrhages of diseased sand smelt, *Atherina boyeri*, in the Gulf of Trieste (NE Adriatic Sea). *Letters in Applied Microbiology*, 54(2), 153–159. <https://doi.org/10.1111/j.1472-765X.2011.03188.x>

Gatesoupe, F. J. (1999). The use of probiotics in aquaculture. *Aquaculture*, 180(1–2), 147–165. [https://doi.org/10.1016/S0044-8486\(99\)00187-8](https://doi.org/10.1016/S0044-8486(99)00187-8)

Hadaidi, G., Röthig, T., Yum, L. K., Ziegler, M., Arif, C., Roder, C., Burt, J., & Voolstra, C. R. (2017). Stable mucus-associated bacterial communities in bleached and healthy corals of *Porites lobata* from the Arabian Seas. *Scientific Reports*, 7(1), 1–11. <https://doi.org/10.1038/srep45362>

Hakim, J. A., Koo, H., Kumar, R., Lefkowitz, E. J., Morrow, C. D., Powell, M. L., & Bej, A. K. (2016). The gut microbiome of the sea urchin, *Lytechinus variegatus*, from its natural habitat demonstrates selective attributes of microbial taxa and predictive metabolic profiles. *FEMS Microbiology Ecology*, 92(9), fiw146. <https://doi.org/10.1093/femsec/fiw146>

Hentschel, U., Piel, J., Degnan, S. M., & Taylor, M. W. (2012). Genomic insights into the marine sponge microbiome. *Nature Reviews Microbiology*, 10(9), 641–654. <https://doi.org/10.1038/nrmicr2839>

Howells, E. J., Vaughan, G., Work, T. M., Burt, J., & Abrego, D. (2020). Annual outbreaks of coral disease coincide with extreme seasonal warming. *Coral Reefs*, 39, 771–781. <https://doi.org/10.1007/s00338-020-01946-2>

Hurtado-McCormick, V., Kahlke, T., Petrou, K., Jeffries, T., Ralph, P. J., & Seymour, J. R. (2019). Regional and microenvironmental scale characterization of the *Zostera muelleri* seagrass microbiome. *Frontiers in Microbiology*, 10, 1011. <https://doi.org/10.3389/fmicb.2019.01011>

Ketchum, R. N., DeBiasse, M. B., Ryan, J. F., Burt, J. A., & Reitzel, A. M. (2018). The complete mitochondrial genome of the sea urchin, *Echinometra* sp. EZ. *Mitochondrial DNA Part B*, 3(2), 1225–1227.

Ketchum, R. N., Smith, E. G., DeBiasse, M. B., Vaughan, G. O., McParland, D., Leach, W. B., & Reitzel, A. M. (2020). Population genomic analyses of the sea urchin *Echinometra* sp. EZ across an extreme environmental gradient. *Genome Biology and Evolution*, 12(10), 1819–1829.

Ketchum, R. N., Smith, E. G., Vaughan, G. O., Phippen, B. L., McParland, D., Al-Mansoori, N., Carrier, T. J., Burt, J. A., & Reitzel, A. M. (2018). DNA extraction method plays a significant role when defining bacterial community composition in the marine invertebrate *Echinometra mathaei*. *Frontiers in Marine Science*, 5, 255. <https://doi.org/10.3389/fmars.2018.00255>

Klindworth, A., Pruesse, E., Schweer, T., Peplies, J., Quast, C., Horn, M., & Glöckner, F. O. (2013). Evaluation of general 16S ribosomal RNA gene PCR primers for classical and next-generation sequencing-based diversity studies. *Nucleic Acids Research*, 41(1), e1–e1. <https://doi.org/10.1093/nar/gks808>

Konopka, A. (2009). What is microbial community ecology? *The ISME Journal*, 3(11), 1223–1230. <https://doi.org/10.1038/ismej.2009.88>

Kurtz, Z. D., Müller, C. L., Miraldi, E. R., Littman, D. R., Blaser, M. J., & Bonneau, R. A. (2015). Sparse and compositionally robust inference of microbial ecological networks. *PLoS Computational Biology*, 11(5), e1004226. <https://doi.org/10.1371/journal.pcbi.1004226>

Li, Y.-F., Xu, J.-K., Chen, Y.-W., Ding, W.-Y., Shao, A.-Q., Liang, X., Zhu, Y.-T., & Yang, J.-L. (2019). Characterization of gut microbiome in the mussel *Mytilus galloprovincialis* in response to thermal stress. *Frontiers in Physiology*, 10, 1086. <https://doi.org/10.3389/fphys.2019.01086>

Li, Y.-F., Yang, N. A., Liang, X., Yoshida, A., Osatomi, K., Power, D., Batista, F. M., & Yang, J.-L. (2018). Elevated seawater temperatures decrease microbial diversity in the gut of *Mytilus coruscus*. *Frontiers in Physiology*, 9, 839. <https://doi.org/10.3389/fphys.2018.00839>

Liew, Y. J., Howells, E. J., Wang, X., Michell, C. T., Burt, J. A., Idaghdour, Y., & Aranda, M. (2020). Intergenerational epigenetic inheritance in reef-building corals. *Nature Climate Change*, 10(3), 254–259. <https://doi.org/10.1038/s41558-019-0687-2>

Lin, X., Hetharua, B., Lin, L., Xu, H., Zheng, T., He, Z., & Tian, Y. (2019). Mangrove sediment microbiome: adaptive microbial assemblages and their routed biogeochemical processes in Yunxiao mangrove national nature reserve, China. *Microbial Ecology*, 78(1), 57–69. <https://doi.org/10.1007/s00248-018-1261-6>

Lokmer, A., & Wegner, K. M. (2015). Hemolymph microbiome of Pacific oysters in response to temperature, temperature stress and infection. *The ISME Journal*, 9(3), 670–682. <https://doi.org/10.1038/ismej.2014.160>

Martino, C., Morton, J. T., Marotz, C. A., Thompson, L. R., Tripathi, A., Knight, R., & Zengler, K. (2019). A novel sparse compositional technique reveals microbial perturbations. *Msystems*, 4(1). <https://doi.org/10.1128/mSystems.00016-19>

McFall-Ngai, M. J., & Ruby, E. G. (1991). Symbiont recognition and subsequent morphogenesis as early events in an animal-bacterial mutualism. *Science*, 254(5037), 1491–1494.

Mortzfeld, B. M., Urbanski, S., Reitzel, A. M., Künzel, S., Technau, U., & Fraune, S. (2016). Response of bacterial colonization in *Nematostella vectensis* to development, environment and biogeography. *Environmental Microbiology*, 18(6), 1764–1781.

Newton, A., Kendall, M., Vugia, D. J., Henao, O. L., & Mahon, B. E. (2012). Increasing Rates of Vibriosis in the United States, 1996–2010: Review of Surveillance Data From 2 Systems. *Clinical Infectious Diseases*, 54(suppl\_5), S391–S395. <https://doi.org/10.1093/cid/cis243>

Oksanen, J., Blanchet, F. G., Kindt, R., Legendre, P., Minchin, P. R., & Ohara, R., Wagner, H., (2013). Package 'vegan'. *Community Ecology Package, Version, 2(9)*, 1–295.

Paparella, F., Xu, C., Vaughan, G. O., & Burt, J. A. (2019). Coral bleaching in the Persian/Arabian Gulf is modulated by summer winds. *Frontiers in Marine Science*, 6, 205. <https://doi.org/10.3389/fmars.2019.00205>

Pita, L., Rix, L., Slaby, B. M., Franke, A., & Hentschel, U. (2018). The sponge holobiont in a changing ocean: from microbes to ecosystems. *Microbiome*, 6(1), 46. <https://doi.org/10.1186/s40168-018-0428-1>

Pollock, J., Glendinning, L., Wisedchanwet, T., & Watson, M. (2018). The madness of microbiome: Attempting to find consensus "best practice" for 16S microbiome studies. *Applied and Environmental Microbiology*, 84, e02627–e2617. <https://doi.org/10.1128/aem.02627-17>

Pootakham, W., Mhantong, W., Yoocha, T., Putchim, L., Sonthirod, C., Naktang, C., Thongtham, N., & Tangphatsornruang, S. (2017). High resolution profiling of coral-associated bacterial communities using full-length 16S rRNA sequence data from PacBio SMRT sequencing system. *Scientific Reports*, 7(1), 1–14. <https://doi.org/10.1038/s41598-017-03139-4>

Popovic, I., & Riginos, C. (2020). Comparative genomics reveals divergent thermal selection in warm-and cold-tolerant marine mussels. *Molecular Ecology*, 29(3), 519–535. <https://doi.org/10.1111/mec.15339>

Quast, C., Pruesse, E., Yilmaz, P., Gerken, J., Schweer, T., Yarza, P., Peplies, J., & Glöckner, F. O. (2012). The SILVA ribosomal RNA gene database project: improved data processing and web-based tools. *Nucleic Acids Research*, 41(D1), D590–D596. <https://doi.org/10.1093/nar/gks1219>

Reshef, L., Koren, O., Loya, Y., Zilber-Rosenberg, I., & Rosenberg, E. (2006). The coral probiotic hypothesis. *Environmental Microbiology*, 8(12), 2068–2073. <https://doi.org/10.1111/j.1462-2920.2006.01148.x>

Reveillaud, J., Maignien, L., Eren, A. M., Huber, J. A., Apprill, A., Sogin, M. L., & Vanreusel, A. (2014). Host-specificity among abundant and rare taxa in the sponge microbiome. *The ISME Journal*, 8, 1198.

Rivera-Pinto, J., Egozcue, J., Pawlowsky-Glahn, V., Paredes, R., Noguera-Julian, M., & Calle, M. (2018). Balances: a New Perspective for Microbiome Analysis. *mSystems*, 3, e00053–18.

Schouw, A., Vulcano, F., Roalkvam, I., Hocking, W., Reeves, E., Stokke, R., Bødtker, G., & Steen, I. (2018). Genome analysis of *Vallitalea guaymasensis* strain L81 isolated from a deep-sea hydrothermal vent system. *Microorganisms*, 6(3), 63. <https://doi.org/10.3390/microorganisms6030063>

Sepulveda, J., & Moeller, A. H. (2020). The effects of temperature on animal gut microbiomes. *Frontiers in Microbiology*, 11, 384. <https://doi.org/10.3389/fmicb.2020.00384>

Shama, L. N., Mark, F. C., Strobel, A., Lokmer, A., John, U., & Mathias Wegner, K. (2016). Transgenerational effects persist down the maternal line in marine sticklebacks: gene expression matches physiology in a warming ocean. *Evolutionary Applications*, 9(9), 1096–1111. <https://doi.org/10.1111/eva.12370>

Shraim, R., Dieng, M. M., Vinu, M., Vaughan, G., McParland, D., Idaghdour, Y., & Burt, J. A. (2017). Environmental Extremes Are Associated with Dietary Patterns in Arabian Gulf Reef Fishes. *Frontiers in Marine Science*, 4, 285. <https://doi.org/10.3389/fmars.2017.00285>

Smith, E. G., Vaughan, G. O., Ketchum, R. N., McParland, D., & Burt, J. A. (2017). Symbiont community stability through severe coral bleaching in a thermally extreme lagoon. *Scientific Reports*, 7(1), 2428. <https://doi.org/10.1038/s41598-017-01569-8>

Smith, P., Willemsen, D., Popkes, M., Metge, F., Gandiwa, E., Reichard, M., & Valenzano, D. R. (2017). Regulation of life span by the gut microbiota in the short-lived African turquoise killifish. *Elife*, 6, e27014.

Sun, Y.-T., Zhou, N., Wang, B.-J., Liu, X.-D., Jiang, C.-Y., Ge, X., & Liu, S.-J. (2019). *Vallitalea okinawensis* sp. nov., isolated from Okinawa trough sediment and emended description of the genus *Vallitalea*. *International Journal of Systematic and Evolutionary Microbiology*, 69(2), 404–410.

Susin, A., Wang, Y., Lê Cao, K.-A., & Calle, M. L. (2020). Variable selection in microbiome compositional data analysis. *NAR Genomics and Bioinformatics*, 2(2), lqaa029. <https://doi.org/10.1093/nargab/lqaa029>

Thissen, D., Steinberg, L., & Kuang, D. (2002). Quick and easy implementation of the Benjamini-Hochberg procedure for controlling the false positive rate in multiple comparisons. *Journal of Educational and Behavioral Statistics*, 27(1), 77–83. <https://doi.org/10.3102/1076986027001077>

Thompson, F. L., Iida, T., & Swings, J. (2004). Biodiversity of Vibrios. *Microbiology and Molecular Biology Reviews*, 68(3), 403–431. <https://doi.org/10.1128/MMBR.68.3.403-431.2004>

Tout, J., Siboni, N., Messer, L. F., Garren, M., Stocker, R., Webster, N. S., Ralph, P. J., & Seymour, J. R. (2015). Increased seawater temperature increases the abundance and alters the structure of natural *Vibrio* populations associated with the coral *Pocillopora damicornis*. *Frontiers in Microbiology*, 6, 432. <https://doi.org/10.3389/fmicb.2015.00432>

Trevathan-Tackett, S. M., Sherman, C. D. H., Huggett, M. J., Campbell, A. H., Laverock, B., Hurtado-McCormick, V., Seymour, J. R., Firle, A., Messer, L. F., Ainsworth, T. D., Negandhi, K. L., Daffonchio, D., Egan, S., Engelen, A. H., Fusi, M., Thomas, T., Vann, L., Hernandez-Agreda, A., Gan, H. M., ... Macreadie, P. I. (2019). A horizon scan of priorities for coastal marine microbiome research. *Nature Ecology & Evolution*, 1–12. <https://doi.org/10.1038/s41559-019-0999-7>

Vargas, S., Leiva, L., & Wörheide, G. (2020). Short-term exposure to high-water temperature causes a shift in the microbiome of the common aquarium sponge *Lendenfeldia chondrodes*. *bioRxiv*.

Vega Thurber, R., Burkepile, D. E., Correa, A. M. S., Thurber, A. R., Shantz, A. A., Welsh, R., Pritchard, C., & Rosales, S. (2012). Macroalgae decrease growth and alter microbial community structure of the reef-building coral *Porites astreoides*. *PLOS One*, 7(9), e44246. <https://doi.org/10.1371/journal.pone.0044246>

Voolstra, C. R., & Ziegler, M. (2020). Adapting with microbial help: Microbiome flexibility facilitates rapid responses to environmental change. *BioEssays*, 42(7), 2000004. <https://doi.org/10.1002/bies.202000004>

Wang, L., Shantz, A. A., Payet, J. P., Sharpton, T. J., Foster, A., Burkepile, D. E., & Vega Thurber, R. (2018). Corals and their microbiomes are differentially affected by exposure to elevated nutrients and a natural thermal anomaly. *Frontiers in Marine Science*, 5, 101. <https://doi.org/10.3389/fmars.2018.00101>

Ward, C. S., Yung, C.-M., Davis, K. M., Blinebry, S. K., Williams, T. C., Johnson, Z. I., & Hunt, D. E. (2017). Annual community patterns are driven by seasonal switching between closely related marine bacteria. *The ISME Journal*, 11(6), 1412–1422. <https://doi.org/10.1038/ismej.2017.4>

Woo, S., Yang, S.-H., Chen, H.-J., Tseng, Y.-F., Hwang, S.-J., De Palmas, S., Denis, V., Imahara, Y., Iwase, F., Yum, S., & Tang, S.-L. (2017). Geographical variations in bacterial communities associated with soft coral *Scleronephthya gracillimum*. *PLoS One*, 12(8), e0183663. <https://doi.org/10.1371/journal.pone.0183663>

Yao, Q., Yu, K., Liang, J., Wang, Y., Hu, B., Huang, X., Chen, B., & Qin, Z. (2019). The composition, diversity and predictive metabolic profiles of bacteria associated with the gut digesta of five sea urchins in Luhuitou fringing reef (northern South China Sea). *Frontiers in Microbiology*, 10, 1168. <https://doi.org/10.3389/fmicb.2019.01168>

Zaneveld, J. R., McMinds, R., & Thurber, R. V. (2017). Stress and stability: applying the Anna Karenina principle to animal microbiomes. *Nature Microbiology*, 2(9), 1–8. <https://doi.org/10.1038/nmicrobiol.2017.121>

Ziegler, M., Grupstra, C. G. B., Barreto, M. M., Eaton, M., BaOmar, J., Zubier, K., Al-Sofyani, A., Turki, A. J., Ormond, R., & Voolstra, C. R. (2019). Coral bacterial community structure responds to environmental change in a host-specific manner. *Nature Communications*, 10(1), 1–11. <https://doi.org/10.1038/s41467-019-10969-5>

Ziegler, M., Seneca, F. O., Yum, L. K., Palumbi, S. R., & Voolstra, C. R. (2017). Bacterial community dynamics are linked to patterns of coral heat tolerance. *Nature Communications*, 8(1), 1–8. <https://doi.org/10.1038/ncomms14213>

Zorz, J. (2019). <https://jkzorz.github.io/2019/06/05/Bubble-plots.html>

## SUPPORTING INFORMATION

Additional supporting information may be found online in the Supporting Information section.

**How to cite this article:** Ketchum, R. N., Smith, E. G., Vaughan, G. O., McParland, D., Al-Mansoori, N., Burt, J. A., & Reitzel, A. M. (2021). Unraveling the predictive role of temperature in the gut microbiota of the sea urchin *Echinometra* sp. EZ across spatial and temporal gradients. *Molecular Ecology*, 30, 3869–3881. <https://doi.org/10.1111/mec.15990>